Large-Scale Atmospheric Forcing Influencing the Long-Term Variability of Mediterranean Heat and Freshwater Budgets: Climatic Indices

FRANCISCO CRIADO-ALDEANUEVA, F. JAVIER SOTO-NAVARRO, AND JESÚS GARCÍA-LAFUENTE

Physical Oceanography Group, Department of Applied Physics II, University of Málaga, Málaga, Spain

(Manuscript received 4 January 2013, in final form 12 November 2013)

ABSTRACT

Interannual to interdecadal precipitation P, evaporation E, freshwater budget ($E - P$), and air–sea net heat flux Q have been correlated with the North Atlantic Oscillation (NAO), eastern Atlantic (EA), eastern Atlantic–western Russia (EA-WR), and Mediterranean Oscillation (MO) climatic indices to explore the influence of atmospheric forcing in the Mediterranean freshwater and heat budget variability. The effect of the MO pattern has similarities with that of the NAO, but MO influence is more intense. On an annual basis, the MO index gives the highest correlation with all the variables considered, and during its negative phase, it exerts a stronger influence than the NAO and is associated with higher P and, especially, enhanced evaporative losses in the Levantine subbasin. The EA pattern does not significantly affect P in the Mediterranean, but a high correlation is found for E and Q from 1979. The EA-WR mode plays a significant role in annual net heat flux since variations in its sign have the potential to induce seesaw variations in the heat budgets of the eastern and western subbasins, as previously found by Josey et al., for wintertime.

1. Introduction

The Mediterranean Sea (Fig. 1), a marginal basin located across a dynamic border that separates two different climatic regions (Europe and North Africa), extends over 3000 km in longitude and over 1500 km in latitude with an area of 2.5×10^{12} m^2, and it connects with the Atlantic Ocean through the Strait of Gibraltar and with the Black Sea through the Turkish Bosphorus and Dardanelles Straits. Semi-enclosed basins such as the Mediterranean are suitable for the characterization of heat and water fluxes since they make a basin budget closure feasible. As evaporation E exceeds precipitation P and river runoff R, inflow from Atlantic through the Strait of Gibraltar is necessary to balance the water and salt budgets.

A great number of studies have dealt with the Mediterranean heat (Bethoux 1979; Bunker et al. 1982; May 1986; Garrett et al. 1993; Gilman and Garrett 1994; Castellari et al. 1998; Matsoukas et al. 2005; Ruiz et al. 2008; Criado-Aldeanueva et al. 2012) and water budgets (Bethoux 1979; Peixoto et al. 1982; Bryden and Kinder 1991; Harzallah et al. 1993; Gilman and Garrett 1994; Castellari et al. 1998; Angelucci et al. 1998; Bethoux and Gentili 1999; Boukthir and Barnier 2000; Mariotti et al. 2002; Mariotti 2010; Romanou et al. 2010; Criado-Aldeanueva et al. 2012), but only in the most recent ones, which use longer datasets, is the attention focused on the interannual variability and its forcing mechanisms. For instance, Criado-Aldeanueva et al. (2012) reported three different periods in the precipitation and evaporation anomalies: from the early 1950s to the late 1960s, a positive trend is observed that changes to negative until the late 1980s, when it changes sign again. This variability is also reflected in the net heat flux exchanged between the ocean and atmosphere and suggests a 40-yr period of multidecadal oscillation related to long-term atmospheric forcing that needs further investigation.

Climatic indices that represent modes of atmospheric variability provide an integrated measure of weather linked more to the overall physical variability of the system than to any individual local variable. Among these indices, the North Atlantic Oscillation (NAO) is one of the most prominent modes of the Northern Hemisphere climate variability [Walker and Bliss 1932; van Loon and Rogers 1978; Barnston and Livezey 1987; see Hurrell et al. (2003) for a recent review]. It consists of a dipole of the sea level pressure over the North Atlantic–European

Corresponding author address: Francisco Criado-Aldeanueva, Dpto. Física Aplicada II, Universidad de Málaga, Campus de Teatinos s/n, 29071 Málaga, Spain.
E-mail: fcaldeanueva@ctima.uma.es

DOI: 10.1175/JHM-D-13-04.1

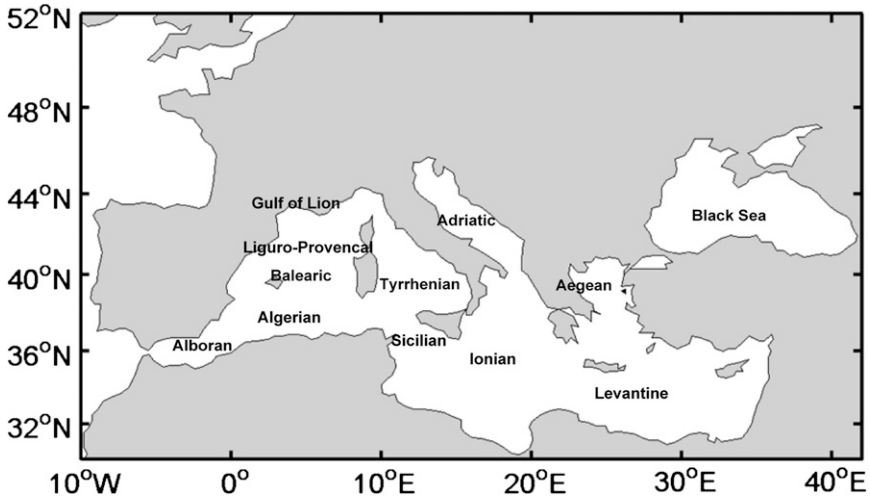

FIG. 1. Map of the Mediterranean Sea. The main basins and subbasins are indicated.

region, with one center reflecting the Iceland low and the other reflecting the Azores high. The positive phase of the NAO (Fig. 2a) is associated with higher sea level pressure average (SLPA) over most parts of Europe and the Mediterranean Sea. The intensification of the Azores high and the deepening of the Icelandic low during this phase strengthens and modifies the orientation of westerlies and associated storm-track activity and leads to drier conditions in southern Europe (south of 45°N) and the Mediterranean and wetter conditions in northern Europe (Walker and Bliss 1932; van Loon and Rogers 1978; Rogers and van Loon 1979; Hurrell 1995; Serreze et al. 1997; Dai et al. 1997; Mariotti et al. 2002; Mariotti and Arkin 2007). Opposite conditions prevail during the negative phase (Fig. 2b), with lower SLPA over southern Europe and the Mediterranean, which leads to higher precipitation in these areas.

The influence of large-scale atmospheric circulation on the climate variability over the Mediterranean region has also been addressed in terms of other teleconnection patterns such as the eastern Atlantic (EA), the eastern Atlantic–western Russia (EA-WR), or the Scandinavian (SCAN) patterns (Josey et al. 2011; Papadopoulos et al. 2012a,b). The positive phase of the EA pattern (Fig. 2c) is dominated by a broad region of anomalously low pressure centered approximately midway of the two centers of the NAO (Josey and Marsh 2005) that gives rise to strong cyclonic wind forcing of the North Atlantic around this location. In its negative state (Fig. 2d), it produces a relatively strong pressure gradient in the western Mediterranean, which can potentially generate a cold northerly airflow and enhanced heat loss in this region (Josey et al. 2011). The EA-WR pattern (Figs. 2e,f) exhibits anomalously high (low) pressure over the North Sea flanked by low (high) pressure centers over western Russia and over the western North Atlantic at 45°–55°N. Positive phases of EA-WR favor northerlies over the eastern Mediterranean and southerlies over the western Mediterranean. The SCAN pattern (not shown) produces weak variations in the SLPA field and plays a minor role in the large-scale atmospheric forcing over the Mediterranean (Josey et al. 2011; Papadopoulos et al. 2012b).

Conte et al. (1989) suggested the possible existence of a Mediterranean Oscillation (MO) associated with dipolar behavior of the atmosphere in the area between the western and eastern Mediterranean. Differences in temperature, precipitation, circulation, and other parameters between both basins were attributed to this MO (Conte et al. 1989; Kutiel et al. 1996; Maheras et al. 1999; Supic et al. 2004), and an index to measure the intensity of this dipole-like behavior was proposed as the normalized 500-hPa height difference anomalies between Algiers (36.4°N, 3.1°E) and Cairo (30.1°N, 31.4°E; Conte et al. 1989). A second version of the index can be calculated based on normalized sea level pressure differences between the Gibraltar northern frontier (36.1°N, 5.3°W) and Ben Gurion Airport, Israel (32.0°N, 34.5°E; Palutikof 2003; data available at www.cru.uea.ac.uk/cru/data/moi), and, more recently, Papadopoulos et al. (2012a,b) introduced the Mediterranean index as the sea level pressure difference between southern France (45°N, 5°E) and the Levantine Sea (35°N, 30°E). Suselj and Bergant (2006) proposed an MO index definition based on EOF analysis of SLPA fields over an extended Mediterranean region, and Gomis et al. (2006) also adopted this definition to study its influence in the flow exchange through Gibraltar. For the reasons given in section 2, we have adopted this EOF-based approach to the MO index for this research.

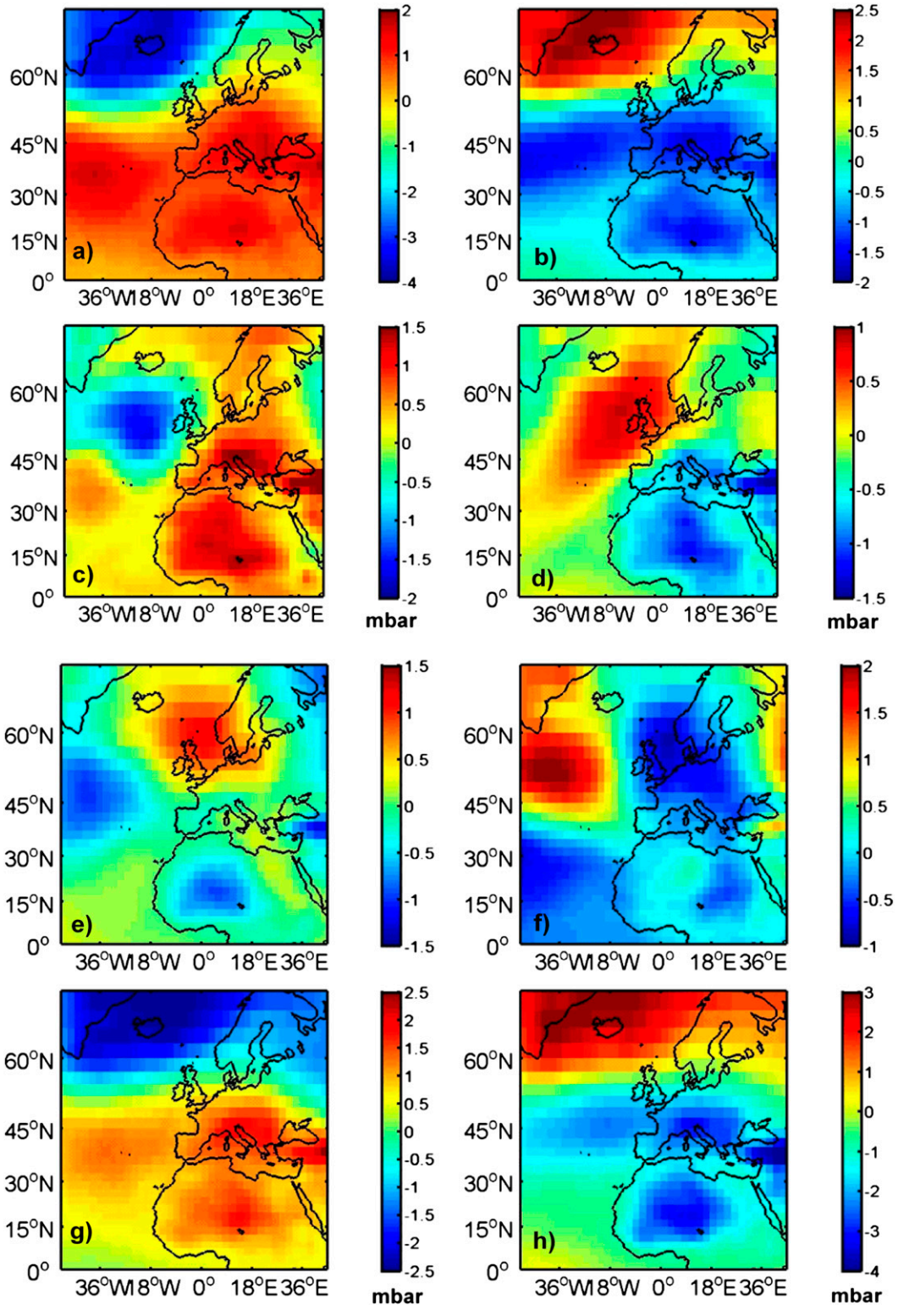

FIG. 2. Composites of sea level pressure anomalies (hPa) in the 1948–2008 period during the (left) positive (higher quartile) and (right) negative (lower quartile) phases of the selected climatic indices: (a),(b) NAO, (c),(d) EA, (e),(f) EA-WR, and (g),(h) MO.

In contrast to NAO, which has been extensively studied, and the other atmospheric indices, only a few previous works focus on the MO index (especially during winter), and more research is required on this topic. This work adds to some of this research by exploring MO influence in annual heat and freshwater budgets in comparison with the other teleconnection patterns. To this aim, we correlate interannual to interdecadal precipitation, evaporation, freshwater budget ($E - P$), and net heat flux Q with several atmospheric climatic indices (NAO, EA, EA-WR, and MO) and analyze the relative importance of their positive and negative phases in the variables. The work is organized as follows: section 2 describes the data and methodology, section 3 presents and discusses the results both from a regional and a global approach, and section 4 summarizes the conclusions.

2. Data and methodology

Since there is no unique way to describe the spatial structure of the low-frequency atmospheric modes of variability, it follows that there is no universally accepted index to describe the temporal evolution of the phenomenon. Climatic indices have been traditionally derived either from the simple difference in surface pressure anomalies or some other climate variable between various locations [see, e.g., Conte et al. (1989), Palutikof (2003), Papadopoulos et al. (2012a,b) for the MO index and Rogers (1984), Hurrell (1995), Jones et al. (1997), Slonosky and Yiou (2001), and Jones et al. (2003) for a comparison between several station-based NAO indices] or from the principal component (PC) time series of the leading EOF of sea level pressure or some other climate variable [Suselj and Bergant 2006; Gomis et al. 2006 for MO index; see Hurrell and Deser (2010) for a review of diverse NAO definitions]. A widely employed analysis of the main modes of atmospheric variability is that carried out at the National Oceanic and Atmospheric Administration (NOAA) Climate Prediction Center (CPC). They characterize the main modes through a rotated principal component analysis (Barnston and Livezey 1987) of the observed monthly-mean 500-hPa height anomaly fields in the region 20°–90°N and provide monthly index values for each mode (see details in www.cpc.ncep.noaa.gov/data/teledoc/teleindcalc.shtml). In this study, we have retrieved CPC monthly index values for the NAO, EA, and EA-WR patterns.

A disadvantage of the station-based indices is that they are fixed in space and are significantly affected by small-scale and transient meteorological events that introduce noise (Trenberth 1984; Hurrell and van Loon 1997), whereas the PC time series approach is a more optimal representation of the full spatial pattern (Hurrell and Deser 2010). For this reason and for homogeneity with the other climatic indices, the MO pattern has been computed as the first EOF mode of normalized sea level pressure anomalies [from the National Centers for Environmental Prediction (NCEP) dataset] across the extended Mediterranean region (30°–60°N, 30°W–40°E), which exhibits a single center located over the central and western Mediterranean (not shown), fairly steady in all seasons. The MO index is then obtained as the corresponding time coefficients of the first EOF mode.

It is important to notice that NAO, EA, and EA-WR can act independently as modes resulting from the same EOF analysis. MO shows some similarity with NAO, with higher-(lower-) than-average SLPA over the Mediterranean during its positive (negative) phase (Figs. 2g,h). On an annual basis, correlation of the MO index with the independent modes of low-frequency variability is 0.57 with NAO and 0.43 with EA (no significant correlation is observed with EA-WR). Seasonally, the summer [July–September (JAS)] MO index is only significantly correlated with NAO ($r = 0.37$), whereas the winter [January–March (JFM)] MO index exhibits a similar correlation ($r \sim 0.33$) with the rest of the indices. Being aware that MO captures, to a certain extent, the influence of the other independent modes (mainly NAO) and hence cannot act independently from them, its potential to more intensely affect the variables over the Mediterranean Sea merits investigation.

Monthly means from January 1948 to February 2009 of precipitation, evaporation, and surface heat fluxes (positive toward the atmosphere, the same as evaporation) have been retrieved from the NCEP–National Center of Atmospheric Research (NCEP–NCAR) reanalysis project (hereafter just NCEP; Kalnay et al. 1996), which is run at T62 spectral resolution (approximately a grid size of 1.9° × 1.9°) with 28 sigma levels. Auxiliary data of monthly-mean sea level pressure at 2.5° × 2.5° for the period 1948–2009 have also been retrieved from NCEP database. Uncertainties derived from the use of reanalysis have been studied by Mariotti et al. (2002), who showed that NCEP data exhibit good agreement when compared with observational P and E datasets at interannual to interdecadal time scales in the Mediterranean area (except for some discrepancies in E in the 1980s and 1990s). For comparison purposes, we have also analyzed monthly data from the Interim European Centre for Medium-Range Weather Forecasts (ECMWF) Re-Analysis (ERA-Interim), the latest reanalysis dataset released by the ECMWF (Berrisford et al. 2009) that focused on the data-rich period since 1979. At 1.5° horizontal resolution, it includes many model improvements, variational bias correction for satellite

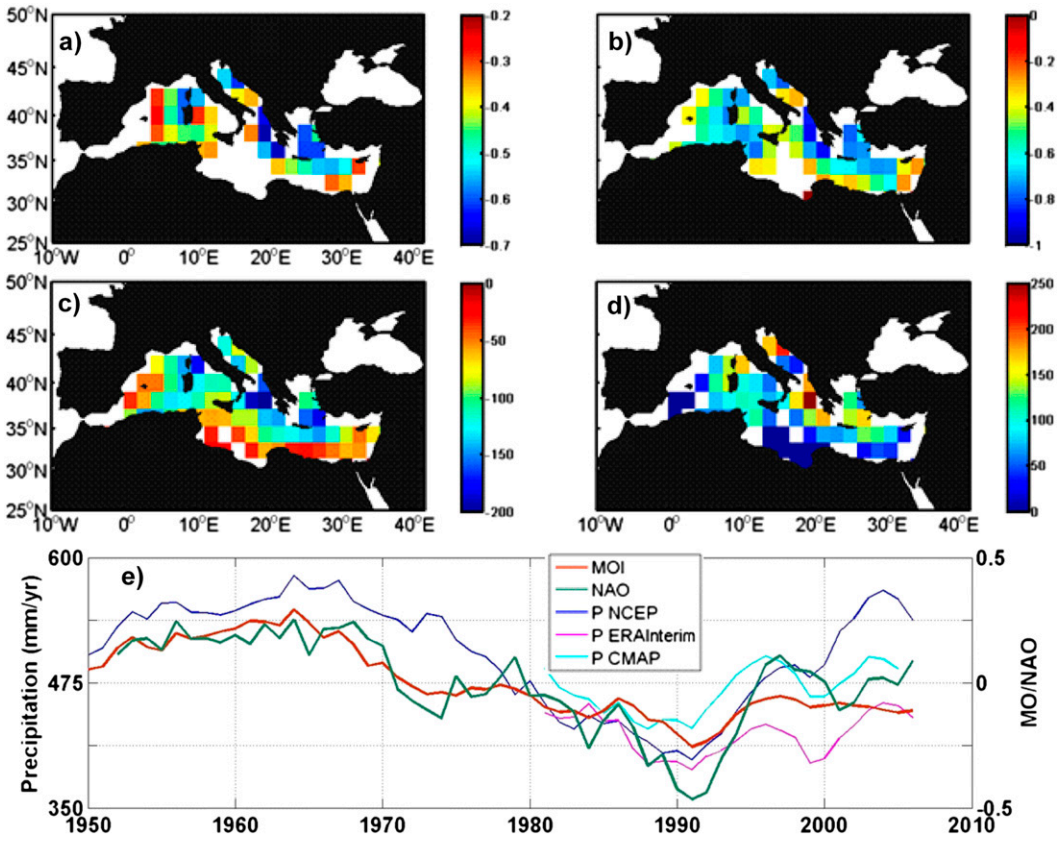

FIG. 3. (a) Correlation (95% significance) between annual P and MO index for the period 1948–2008. (b) Correlation (95% significance) between 5-yr running means of P and MO index for the period 1948–2008. (c) Composite of P anomalies (mm yr^{-1}) under the positive (higher quartile) phase of MO index. (d) Composite of P anomalies (mm yr^{-1}) under the negative (lower quartile) phase of MO index. (e) Time series of 5-yr running means of Mediterranean-averaged P and the most correlated NAO and MO climatic indices.

data, and other improvements in data handling. ERA-Interim uses mostly the sets of observations acquired for the 40-yr ECMWF Re-Analysis (ERA-40) supplemented by data for the most recent years from the ECMWF operational archive. Reasonably good agreement has been observed between these two reanalysis datasets in their common period both in the seasonal cycles (not shown) and in the interannual variability (Figs. 3e, 4e, 5e, 6e). Because of the longer time coverage provided by NCEP, results will focus on this dataset, but comparisons with ERA-Interim will be also discussed.

Although the use of reanalysis allows the construction of homogeneous time series (both in time and space) and leads to a better representation of the basin-scale features, validation with observational datasets is desirable for robustness. For this reason, data from the CPC Merged Analysis of Precipitation (CMAP; Xie and Arkin 1996, 1997) have also been retrieved and analyzed. This dataset gives estimation of monthly-mean precipitation at 2.5° × 2.5° resolution for the period 1979–2009. The standard version consists of a merged analysis, mainly based on gauge stations over land and satellite estimates over the ocean, which matches reasonably well the reanalysis outputs in their common period, especially in terms of interannual variability (Fig. 3e), thus reinforcing reliability of our results.

Linear correlation maps have been used to identify coupled patterns between the variables and the atmospheric indices. The statistical significance of the correlation has been computed by transforming the correlation matrix in a Student's t-test distribution with $N - 2$ degrees of freedom, where N is the number of elements of the analyzed time series. Time filtering into low- and high-frequency components is achieved using a 5-yr running mean to take into account the long-time-scale effects of the indices. Composite analysis (anomalies of the variables with respect to the climatic mean over 1948–2009 have been selected for the analysis) was also performed to highlight the differences between the positive and negative phases of the indices, defined as the upper and

lower quartiles of the climatic indices time series over the period 1948–2009. Only the points where the results are statistically different from zero (according to a Student's *t* test at 95% significance) have been represented.

3. Results and discussion

a. Precipitation

Table 1 shows the correlation between precipitation and the climatic indices for the several datasets analyzed. On an annual basis, the MO index shows the highest (negative) correlation ($r = 0.45$ on average over 56% of the Mediterranean) with values up to −0.7 in the Aegean and northern Levantine subbasins (Fig. 3a). The correlation increases in winter (or if the entire rainy period, from October to March, is considered), when P is generally linked to storm-track activity captured by atmospheric indices, with wide regions close to −0.6 (not shown). In summer, most of the precipitation across the Mediterranean region is of convective origin and is poorly correlated with the large-scale atmospheric forcing. At decadal time scales (5-yr running means), MO and NAO have a similar performance ($r = 0.56$, on average) and up to 80% of the basin (except the southern Ionian and westernmost areas) is significantly correlated (Fig. 3b). EA and EA-WR exhibit lower correlation with P, and only some isolated regions are sensitive to their effect (see Table 1). Correlation is rather similar for different datasets but is fairly dependent on the period analyzed (this makes the 60-yr NCEP time series the most reliable for long-term variability): if only the period from 1979 is considered (ERA-Interim, $NCEP_{79–09}$, and CMAP data), correlation between the MO index and P is weaker in general since departure from both time series is evident, especially from 2000 but also in the 1980s (Fig. 3e).

Negative correlation of P with NAO (and MO, see the similarity between their SLPA fields in Fig. 2) is a well-documented feature because its positive phase (stronger dipole) produces an SLPA field (Fig. 2a) that strengthens and modifies the orientation of prevailing westerly winds and associated storm-track activity, which causes dry anomalies in the Mediterranean region (Hurrell 1995; Serreze et al. 1997; Dai et al. 1997; Mariotti et al. 2002; Mariotti and Arkin 2007). The negative phase (especially that of MO, with higher anomalies in the SLP field) is linked to an intense cyclogenesis over the central/western Mediterranean that produces anomalously wet conditions over most of the basin and, hence, negative correlation with P. Precipitation anomalies during the positive and negative phases (higher and lower quartiles) of the indices are shown in Table 2. The MO

TABLE 1. Mean absolute correlation at 95% significance level between annual and decadal (5-yr running means) climatic indices and P, E, $E - P$, and Q. The fraction of grid points significantly correlated is shown in parentheses. The last column displays the correlation (n.s. indicates that correlation is not significant) between the selected indices and the Mediterranean-averaged variables at decadal (5-yr running means) time scale (time series in Figs. 3e, 4e, 5e, 6e). Boldface indicates the strongest influence.

	Annual means				5-yr means				5-yr Mediterranean averaged			
	NAO	MO	EA	EA-WR	NAO	MO	EA	EA-WR	NAO	MO	EA	EA-WR
P_{NCEP}	0.31 (33%)	**0.45 (56%)**	0.37 (35%)	0.31 (3%)	0.55 (87%)	**0.56 (81%)**	0.50 (55%)	0.39 (35%)	**−0.82**	−0.76	−0.43	n.s.
$P_{ERA\text{-}I}$	0.42 (12%)	0.46 (21%)	n.s.	0.41 (7%)	0.61 (42%)	0.57 (37%)	0.54 (37%)	0.57 (39%)	−0.57	−0.49	n.s.	−0.40
$P_{79–09}$	0.41 (22%)	0.42 (26%)	0.40 (6%)	n.s.	0.62 (81%)	0.54 (56%)	0.65 (74%)	0.54 (60%)	−0.74	−0.54	0.79	−0.56
P_{CMAP}	0.47 (31%)	0.51(26%)	0.44 (4%)	0.39 (4%)	0.61 (57%)	0.60 (40%)	0.54 (40%)	0.56 (21%)	−0.77	−0.60	n.s.	n.s.
E_{NCEP}	0.33 (37%)	**0.36 (40%)**	0.32 (10%)	0.33 (21%)	**0.52 (79%)**	0.52 (56%)	0.42 (49%)	0.45 (42%)	**−0.60**	−0.45	n.s.	n.s.
$E_{ERA\text{-}I}$	0.40 (15%)	0.40 (4%)	0.45 (24%)	0.42 (28%)	0.59 (89%)	0.50 (58%)	0.74 (91%)	0.57 (64%)	−0.68	−0.50	0.87	−0.53
$E_{79–09}$	0.42 (44%)	0.38 (5%)	0.45 (15%)	0.41 (13%)	0.63 (86%)	0.48 (56%)	0.64 (95%)	0.48 (31%)	−0.65	−0.41	0.70	n.s.
$E - P_{NCEP}$	0.30 (15%)	**0.39 (38%)**	0.35 (33%)	0.33 (23%)	0.42 (59%)	0.48 (59%)	**0.51 (65%)**	0.42 (42%)	n.s.	n.s.	**0.59**	n.s.
$E - P_{ERA\text{-}I}$	0.41 (13%)	0.44 (10%)	0.42 (6%)	0.44 (9%)	0.55 (61%)	0.53 (32%)	0.70 (72%)	0.54 (44%)	−0.46	n.s.	0.85	−0.37
$E - P_{79–09}$	0.43 (17%)	0.43 (8%)	0.41 (9%)	0.41 (6%)	0.57 (44%)	0.55 (19%)	0.62 (55%)	0.54 (49%)	n.s.	n.s.	0.68	n.s.
Q_{NCEP}	0.37 (51%)	**0.37 (59%)**	0.31 (24%)	0.36 (26%)	0.58 (76%)	**0.58 (83%)**	0.40 (49%)	0.52 (43%)	**−0.68**	−0.63	n.s.	0.39
$Q_{ERA\text{-}I}$	0.41 (22%)	0.39 (4%)	0.42 (20%)	0.43 (34%)	0.58 (79%)	0.51 (44%)	0.68 (83%)	0.58 (66%)	−0.70	−0.51	0.83	−0.56
$Q_{79–09}$	0.46 (54%)	0.41 (6%)	0.44 (13%)	0.43 (17%)	0.64 (95%)	0.49 (54%)	0.65 (86%)	0.50 (21%)	−0.65	−0.41	0.69	n.s.

exerts the strongest influence with precipitation anomalies close to 100 mm yr^{-1} on average over most of the basin. Higher anomalies are observed in the northern Mediterranean in both phases, with values up to −200 mm yr^{-1} during the positive phase in the Ionian and Levantine subbasins and up to 250 mm yr^{-1} during the negative phase in the Ionian and northern Adriatic (see Figs. 3c,d). All indices result in precipitation anomalies of similar sign across the basin (see Table 2), except the positive EA phase that produces a dipole response with positive (negative) anomalies in some areas of the eastern (western) basin.

Basinwide decadal to interdecadal variability of the Mediterranean precipitation (Fig. 3e) appears to be even more closely related to NAO and MO indices with correlations of −0.82 and −0.76, respectively (Table 1). In particular, the decrease from the mid-1960s to early 1990s corresponds to a switch from a low to a high state of the indices (notice that −NAO and −MO indices have been plotted). These results are in good agreement with those of Mariotti et al. (2002), who obtained (only for NAO) a correlation of −0.51 and −0.84 for annual and decadal (5-yr running means) variability, respectively, and confirmed the importance of the choice of a long period for budget studies in the Mediterranean, since the long-time-scale effects of the indices must be taken into account because of their direct implication on the variables (Pettenuzzo et al. 2010).

b. *Evaporation*

On an annual basis, the MO index also presents the strongest correlation (r = −0.36, on average; Table 1) with evaporation, although only some areas of the Levantine (with stronger negative correlation, r close to −0.6) and western subbasins are significantly correlated (Fig. 4a). NAO performs a rather similar influence (r = 0.33, on average, over 37% of the Mediterranean), whereas EA and EA-WR seem to be poorly correlated with evaporation. At decadal time scales (5-yr running means), NAO and MO show the same correlation (r = 0.52, on average), although NAO affects more extensive areas, especially the Liguro–Provençal, south of Greece (with values close to −0.8), and Levantine subbasins (Fig. 4b). It is interesting to note that the MO influence extends to almost 80% of the basin (with similar correlation values) if the summer index is considered. Since evaporation is higher in autumn (Mariotti et al. 2002; Romanou et al. 2010; Criado-Aldeanueva et al. 2012), it could be argued that the atmospheric forcing in summer preconditions, to a certain extent, its evolution in the following months. From 1979, higher correlation is observed for most indices, especially EA with r above 0.7 over more than 90% of the Mediterranean.

TABLE 2. Mediterranean-averaged anomalies in the 1948–2008 period during the positive [composite anomaly (CA)+, higher quartile] and negative (CA-, lower quartile) phases of the selected climatic indices (NAO, MO, EA, and EA-WR). Anomalies of opposite sign across the basin are separated by a slash mark. The fraction of points where the anomaly is significantly different from zero is shown in parentheses. The spatial pattern of results highlighted in boldface is shown in the corresponding figures.

	NAO		MO		EA		EA-WR	
	CA+	CA−	CA+	CA−	CA+	CA−	CA+	CA−
P_{NCEP} (mm yr^{-1})	−83.1 (85%)	58.3 (62%)	**−93.0 (91%)**	**86.9 (78%)**	87.8/−39.4 (65%)	58.8 (79%)	37.6 (37%)	46.1 (49%)
E_{NCEP} (mm yr^{-1})	**−91.7 (92%)**	46.6 (41%)	−68.1 (78%)	**98.1 (74%)**	79.2 (81%)	37.3 (53%)	66.2/−36.4 (59%)	43.7/−78.3 (59%)
$E - P_{NCEP}$ (mm yr^{-1})	74.3/−74.2 (63%)	57.4/−90.5 (51%)	75.1/−58.2 (73%)	**119.7/−89.3 (79%)**	88.2/−81.1 (77%)	**−65.7 (67%)**	60.8/−47.7 (49%)	51.4/−78.8 (45%)
Q_{NCEP} (W m^{-2})	−11.4 (91%)	5.5 (46%)	−8.4 (86%)	11.1 (86%)	8.1/−5.9 (67%)	**4.9 (54%)**	**9.4/−3.8 (70%)**	5.7/−10.1 (74%)

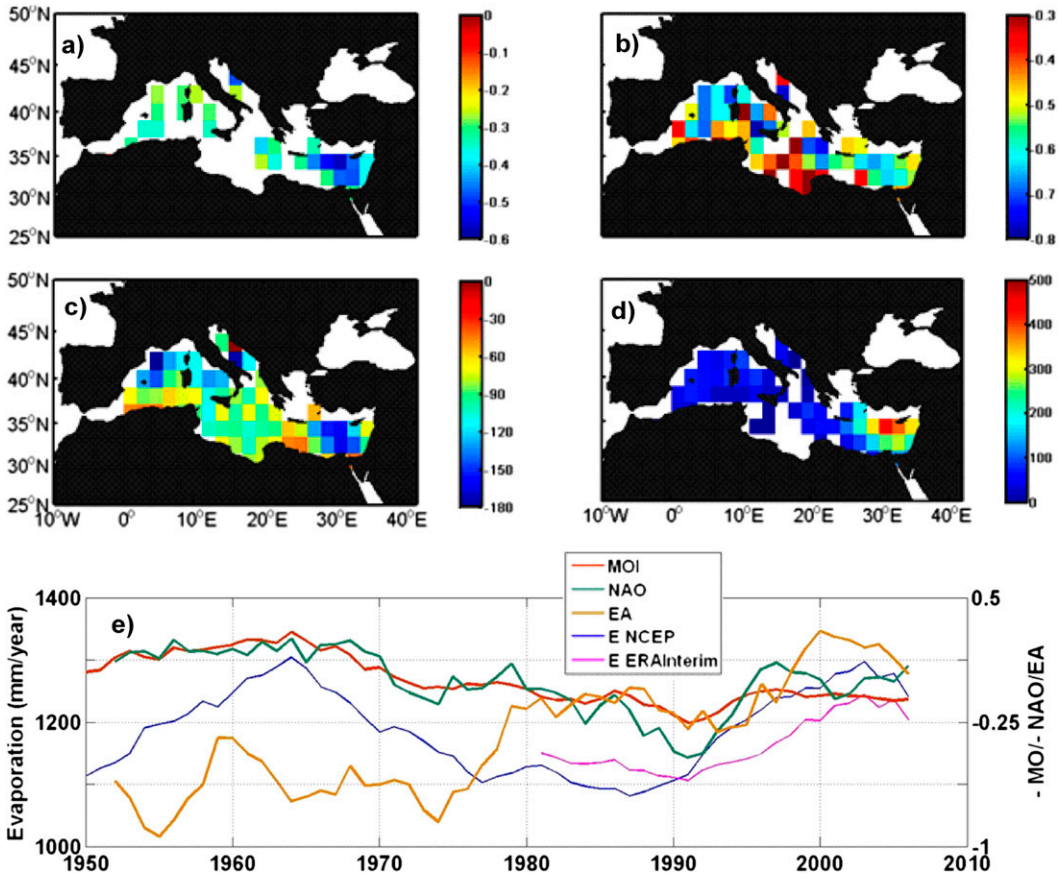

FIG. 4. (a) Correlation (95% significance) between annual E and MO index for the period 1948–2008. (b) Correlation (95% significance) between 5-yr running means of E and NAO index for the period 1948–2008. (c) Composite of E anomalies (mm yr^{-1}) under the positive (higher quartile) phase of NAO index. (d) Composite of E anomalies (mm yr^{-1}) under the negative (lower quartile) phase of MO index. (e) Time series of 5-yr running means of Mediterranean-averaged E and the selected NAO, MO, and EA climatic indices.

Anticorrelation for MO (and NAO) is again expected since, in its negative phase, anomalously low pressure over the whole basin is observed (see Fig. 2h). This favors colder and drier air masses from central Europe that generate more severe weather conditions over the northern and eastern Mediterranean and, hence, an intensification of evaporative losses to the atmosphere. Conversely, the positive MO phase is associated with higher-than-average pressure over the Mediterranean and North Africa (Fig. 2g) that promotes a shift of the wind trajectories toward lower latitudes. Warmer and moister air masses are then conveyed toward the Mediterranean, leading to milder winters and a consequent decrease in the evaporative loss, similar to that shown by Hurrell (1995) for the NAO.

Negative evaporation anomalies are higher under the positive NAO phase (-92 mm yr^{-1} on average over most of the basin; see Table 1) with values up to -160 mm yr^{-1} in the Levantine basin and the Gulf of Lion (Fig. 4c), two well-documented sites of formation of Levantine Intermediate Water (LIW) and Western Mediterranean Deep Water (WMDW), respectively. This decrease in evaporation (and associated latent heat losses) may be reflected in a reduction of the intermediate and deep waters formed [see Josey (2003) and Papadopoulos et al. (2012a) for a complete discussion of the winter convection processes]. As for precipitation, the negative MO phase exerts stronger influence and leads to higher (positive) evaporation anomalies (98 mm yr^{-1} on average; Table 1), with values above 400 mm yr^{-1} in the Levantine subbasin (Fig. 4d). In this phase, the dipole of anomalously low pressure over central Europe and Turkey (Fig. 2h) brings colder and drier air masses from continental regions to the Levantine subbasin, which enhance evaporative losses in this area and may promote winter LIW formation. All indices result in evaporation anomalies of similar sign across the basin (see Table 2),

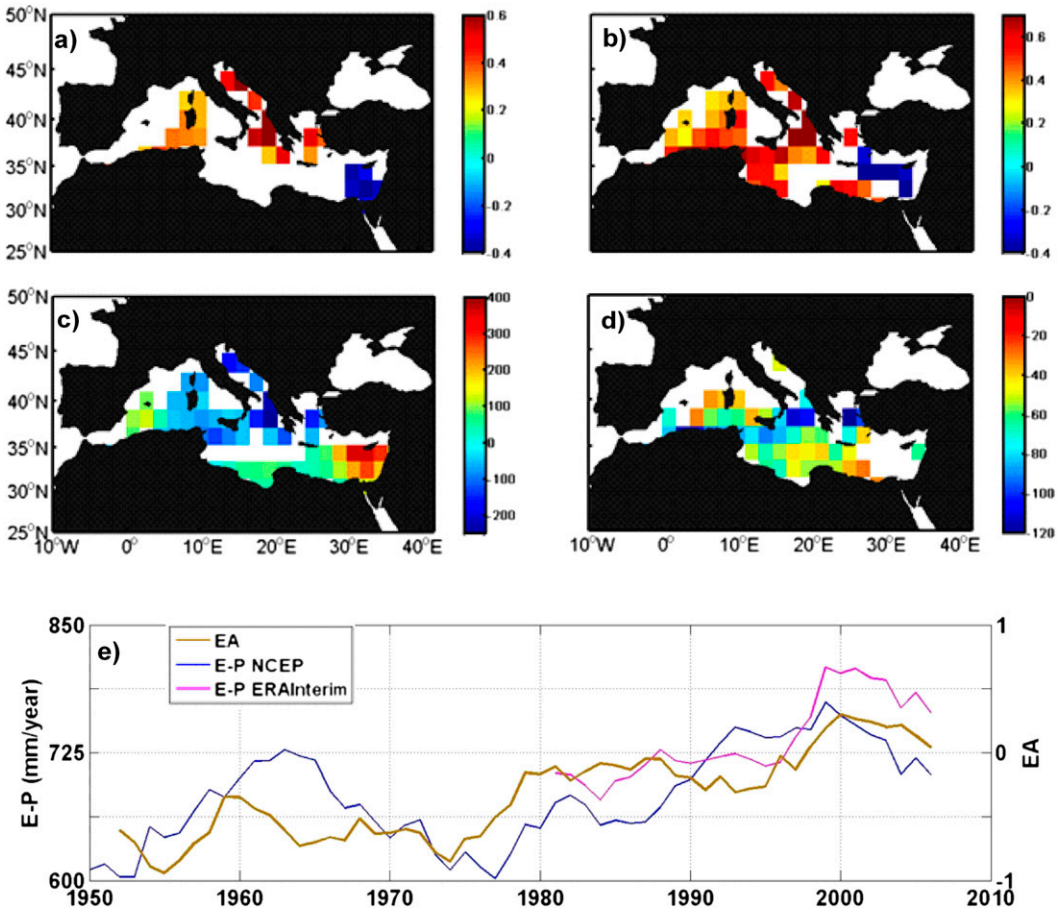

FIG. 5. (a) Correlation (95% significance) between annual $E - P$ and MO index for the period 1948–2008. (b) Correlation (95% significance) between 5-yr running means of $E - P$ and EA index for the period 1948–2008. (c) Composite of $E - P$ anomalies (mm yr^{-1}) under the negative (lower quartile) phase of MO index. (d) Composite of $E - P$ anomalies (mm yr^{-1}) under the negative (lower quartile) phase of EA index. (e) Time series of 5-yr running means of Mediterranean-averaged $E - P$ and the most correlated EA climatic index.

except the EA-WR pattern, which produces a dipole response with positive (negative) anomalies in most of the eastern (western) basin in the positive phase and vice versa in the negative phase. This behavior will be described in detail for the net heat flux in section 3d.

Basinwide decadal to interdecadal variability of the Mediterranean evaporation (Fig. 4e) is well correlated with the NAO index ($r = -0.6$; Table 1), but not significantly with EA or EA-WR (in the case of EA-WR, because it produces correlation of a different sign in the eastern and western subbasins). Correlation increases from 1979 (ERA-Interim, NCEP$_{79–09}$), and a very good agreement between the EA time series and basin-averaged evaporation (Fig. 4e) is found ($r = 0.87$ and 0.7, respectively). However, this increase is more likely to be related to the shorter period analyzed, which coincided with an agreement of both time series in contrast to the departure observed before 1979.

c. $E - P$ freshwater budget

The freshwater budget ($E - P$) is the combination of the two above contributions (E and P). On an annual basis, the MO index gives correlation of different signs in the easternmost Levantine subbasin (negative correlation up to -0.4) and some areas of the Adriatic, the Ionian, the Aegean, and the western subbasin near Corsica and Sardinia (positive correlation up to 0.8; Fig. 5a). However, only 38% of the Mediterranean is significantly correlated with this index (Table 1). The spatial pattern correlation of EA is rather similar to that of MO ($r = 0.35$ on average), whereas NAO and EA-WR are not significantly correlated in most of the basin. From 1979, the correlation with all climatic indices tends to increase, but the fraction of points significantly correlated is lower. At decadal time scales (5-yr running means), this bimodal pattern becomes more

evident, with significant positive correlation almost everywhere (higher values up to 0.8 in the Adriatic and northern Ionian) and negative correlation restricted to the easternmost Levantine subbasin (Fig. 5b for EA and similarly for MO and NAO, the latter with lower correlation values). For the most recent decades, a fairly good correlation is found with EA ($r = 0.7$, on average, from ERA-Interim data over more than 70% of the basin).

The $E - P$ anomalies under the positive and negative phases of the indices also follow this bimodal pattern as a consequence of the different sensitiveness of E and P to the atmospheric forcing in each region. Again, the negative phase of the MO index exerts the strongest influence (Table 2), with positive anomalies up to 400 mm yr^{-1} in the Levantine subbasin and negative anomalies about -200 mm yr^{-1} above 35°N (Fig. 5c). As shown in Figs. 3d and 4d, the negative phase of MO is associated with intense (positive) evaporation anomalies and a minor increase in precipitation in the Levantine basin that results in this $E - P$ pattern. In contrast, north of 35°N, the noticeable precipitation increase (Fig. 3d) and the reduced changes in evaporation (Fig. 4d) result in a negative $E - P$ anomaly (Fig. 5c). Opposite conditions prevail during the positive MO phase: negative anomalies in the Levantine basin and positive anomalies north of 35°N (not shown), with more moderate values (Table 2). A rather similar spatial pattern is observed for NAO (see Table 2 for average values), but the fraction of points significantly influenced is lower. EA-WR also affects $E - P$ in a dipolar manner, but in this case, E is dominant, and changes in $E - P$ closely follow those of E [positive (negative) anomalies in some areas of the eastern (western) basin in the positive phase and vice versa]. The only exception to this bimodal pattern is associated with the negative EA phase that produces negative $E - P$ anomalies in most of the basin (Fig. 5d). In this state, precipitation anomalies are higher than those of evaporation, except in the Levantine and northwestern subbasins, where they tend to compensate and result in nonsignificant $E - P$ changes (Fig. 5d).

Mediterranean-averaged decadal to interdecadal $E - P$ variability (Fig. 5e) is not significantly correlated with MO, NAO, and EA-WR because of this bimodal pattern of correlation of opposite sign. EA shows a reasonably good correlation ($r = 0.59$; Table 2) that increases if only the period from 1979 is considered ($r = 0.85$ from ERA-Interim data), because the 1960s decade of high discrepancy has been left out.

d. Net heat flux

The net air–sea heat flux is the sum of the two radiation components (solar shortwave radiation absorbed by the sea and longwave radiation emitted by the sea) and the two turbulent terms (latent and sensible heat). Annual net heat flux is moderately correlated (r close to 0.4 on average; Table 1) with MO index (Fig. 6a) in most parts of the Mediterranean (except the Alboran, Adriatic, and north Aegean subbasins, where correlation is not significant). Similar results are found for NAO index, but more extended areas (especially the southern Ionian, not shown) are not significantly correlated, whereas for EA and EA-WR only approximately 25% of the basin is significantly correlated on an annual basis (Table 1). Decadal variations (5-yr running means) are more correlated with the atmospheric indices, especially with MO (r up to -0.9 off Sicily and the south of Greece and close to -0.7 in most of the Levantine basin; Fig. 6b).

As shown by Criado-Aldeanueva et al. (2012), the net heat flux variability is mostly determined by the latent heat variability, with this contribution becoming the main source of interannual variability. Since latent heat is directly related to evaporation, similarity between Figs. 4a,b and 6a,b is expected. However, stronger correlation is observed with NAO and MO for net heat flux (see also Table 1) because of the contribution of the other components that correlate well with these indices. Notice that the sign of the correlation is negative because we have selected net heat flux positive toward the atmosphere (the same as evaporation).

We can now compare these results with those of Papadopoulos et al. (2012a), who correlate latent and sensible heat fluxes [from Objectively Analyzed Air–Sea Fluxes (OAFlux)] (Yu et al. 2008) with several climatic indices (the four in this study, among others) during winter (November–March). For the net heat flux, we find, on an annual basis, a higher correlation with NAO index ($r = 0.37$, on average, compared to their $r \sim 0.2$) and a minor fraction of points influenced by EA-WR (26% compared to their ~60%). They also report a positive correlation with MO index in the westernmost Balearic and Alboran subbasins that has not been found on an annual basis. But, the most outstanding difference is related to EA pattern: on an annual basis, only about 25% of the Mediterranean is significantly correlated with EA index (Table 1), but during winter, its influence extends to most of the basin (with r up to 0.6) and plays a significant role in the heat loss associated with intermediate and deep water formation processes (Josey et al. 2011; Papadopoulos et al. 2012a,b). Despite the different datasets and time periods analyzed, these changes are likely related to the seasonal variability of the EA pattern that is enhanced during wintertime and weakens in spring and summer (Barnston and Livezey 1987; Rogers 1990).

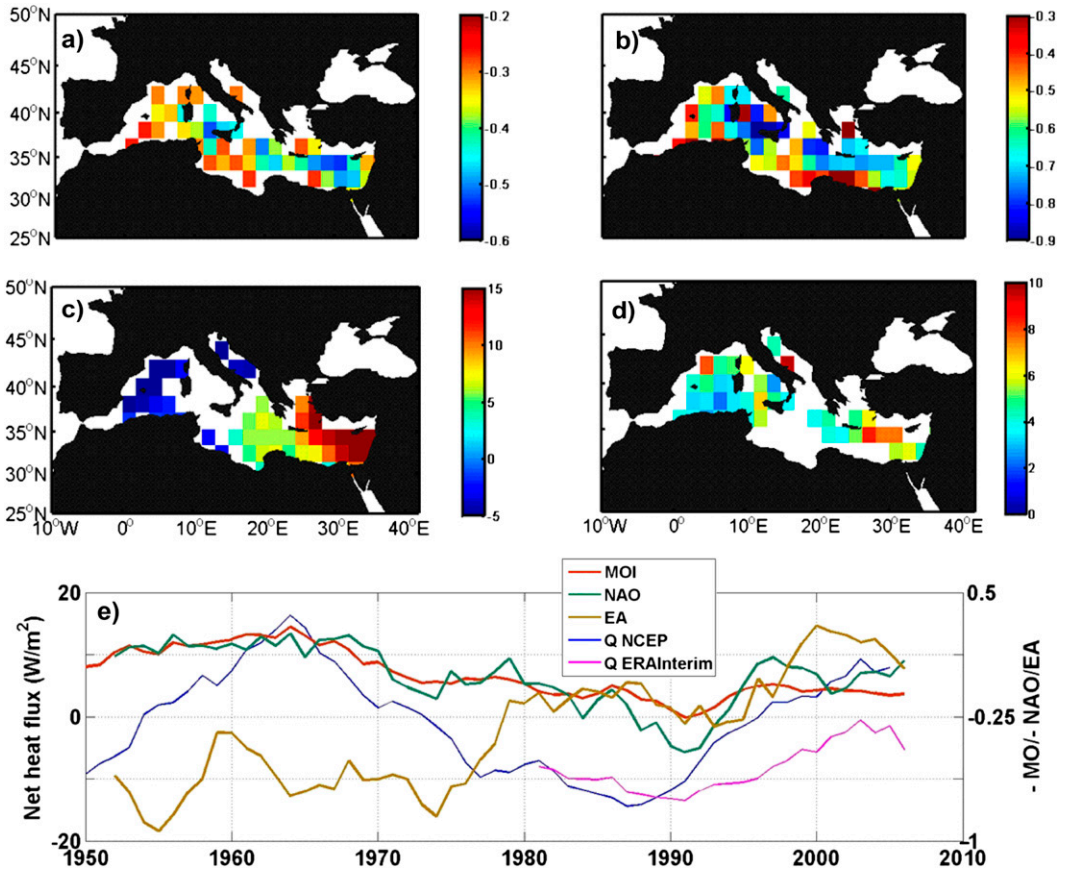

FIG. 6. (a) Correlation (95% significance) between annual Q and MO index for the period 1948–2008. (b) Correlation (95% significance) between 5-yr running means of Q and MO index for the period 1948–2008. (c) Composite of Q anomalies ($W\,m^{-2}$) under the positive (higher quartile) phase of EA-WR index. (d) Composite of Q anomalies ($W\,m^{-2}$) under the negative (lower quartile) phase of EA index. (e) Time series of 5-yr running means of Mediterranean-averaged Q and the selected NAO, MO, and EA climatic indices.

Negative net heat flux anomalies over the entire Mediterranean Sea are associated with the positive NAO and MO phases (Table 2) because of a higher shortwave radiation and lower sensible and, especially, latent losses (i.e., −2.5, +1.2, −2.9, and −7.2 $W\,m^{-2}$ for shortwave, longwave, sensible, and latent terms, respectively, in the positive NAO phase). Opposite conditions prevail in the negative MO phase, with positive heat anomalies all across the basin mainly due to higher evaporative losses (5.4, −3.4, 2.2, and 6.9 $W\,m^{-2}$ for shortwave, longwave, sensible, and latent terms, respectively) that become more important in the Levantine basin (Fig. 4d; an explanation for this is provided in section 3b).

Since latent heat variability regulates the net heat flux variability, the spatial patterns of net heat anomalies in the positive and negative NAO and MO phases are similar to those of evaporation (Figs. 4c,d) and will not be repeated here. Instead, we will discuss now the influence of EA and EA-WR to compare with previous works that perform a similar analysis for wintertime. The negative EA phase (Fig. 6d) is associated with positive net heat anomalies in the western basin (up to 8–10 $W\,m^{-2}$) and some areas of the Levantine subbasin with values higher than 8 $W\,m^{-2}$. However, anomalies are significantly different from zero only in 54% of the Mediterranean, and the spatially averaged net heat anomaly is about 5 $W\,m^{-2}$ (Table 2). As shown in Fig. 2d, in the negative EA phase, higher-than-average SLPA over the British Isles induces northeasterly flow of cold dry air, which steepens the sea–air temperature and humidity gradients, thus favoring stronger-than-normal heat loss over the entire basin. The influence of EA pattern in enhanced heat losses is similar to that of NAO (~5.5 $W\,m^{-2}$ in 46% of the basin; Table 2), but both are less than half of MO. Josey et al. (2011) found a stronger effect of EA pattern in winter heat losses and a minor impact of NAO (they did not consider the MO pattern). Since they also analyzed the NCEP dataset in a similar time period (1958–2006), differences are likely

to be attributable to the seasonality of the atmospheric patterns. The enhanced EA high (in its negative state) and a slight shift to the east during winter may lead to a much stronger influence over the whole basin in this season.

The EA-WR mode generates net heat anomalies of opposite sign in the eastern and western subbasins. In its positive state, positive anomalies (mainly associated to higher latent losses) are found in the eastern subbasin with values up to 15 W m^{-2} in the Levantine area, whereas negative anomalies (due to lower latent losses) are located in the Adriatic and Balearic subbasins with more moderate values (~5 W m^{-2}). This dipolar pattern can be explained based on the SLPA associated with the positive EA-WR phase (Fig. 2e): the higher-than-average SLPA over northern Europe induces a northerly flow of cold dry air over the eastern basin, but a southerly flow of relatively warm moist air over the western basin leads to net heat anomalies of different sign. Opposite conditions prevail during the negative phase, and thus, variations in the sign of EA-WR have the potential to induce seesaw variations in the heat budgets of the eastern and western basins, as shown by Josey et al. (2011), who found a strong impact of this mode in winter heat fluxes.

Basinwide decadal to interdecadal Mediterranean net heat flux variability (Fig. 6e) is well correlated with NAO and MO indices ($r = -0.68$ and -0.63, respectively). As previously noted, the bimodal pattern associated with EA-WR prevents a good correlation when Mediterranean-averaged net heat is considered. Similarly to evaporation (remember that this term is the main source of interannual net heat variability), a very good correlation with EA is found from 1979 ($r = 0.83$ from ERA-Interim and 0.69 from $NCEP_{79–09}$; see also Fig. 6e).

4. Summary and concluding remarks

We have correlated interannual to interdecadal precipitation, evaporation, freshwater budget ($E - P$), and net heat flux with the climatic indices NAO, EA, EA-WR, and MO to explore the influence of atmospheric forcing in the variability of the Mediterranean freshwater and heat budgets. A composite analysis to highlight the differences between the positive and negative phases of the indices and hence to determine the cause–effect relationships between them has also been performed. Although NAO and MO show, in general, a similar influence on the Mediterranean, some differences are worth mentioning: (i) on annual basis, MO index gives the highest correlation with all the variables considered (Table 1), and (ii) particularly during its negative phase, MO exerts a stronger influence than NAO and is associated with higher precipitation and, especially, evaporative losses in the Levantine basin.

Both NAO and MO induce precipitation anomalies of the same sign all across the basin, and the Mediterranean-averaged precipitation decrease from the mid-1960s to the early 1990s clearly corresponds to a switch from a negative to a positive phase of both indices. For evaporation, their influence is more pronounced in the Levantine basin, with positive anomalies (and associated latent heat losses) during the negative phase. Specifically, the different sensitivities of E and P across the Mediterranean lead to correlations of opposite sign for $E - P$ in the easternmost area with respect to the rest of the basin. The EA pattern does not significantly affect P in the Mediterranean, but a high correlation is found for E and net heat from 1979 that is worth noting. The strong effect of this mode in winter heat losses reported by Josey et al. (2011) is not so evident on an annual basis because of the seasonality of the EA pattern that weakens in spring and summer (Barnston and Livezey 1987; Rogers 1990). In contrast, the EA-WR mode plays a significant role in generating net heat anomalies of opposite sign in the eastern and western subbasins, as previously found by Josey et al. (2011).

In conclusion, taking into account that MO is not independent of the other modes of low-frequency variability (especially from NAO, $r = 0.57$ on an annual basis), we have shown its potential to more intensely affect the variables over the Mediterranean Sea and to provide a valuable measure of the atmospheric impact on the basin, thus becoming a powerful tool for monitoring the variability of the heat and freshwater budgets.

Acknowledgments. This work has been carried out in the frame of the P07-RNM-02938 Junta de Andalucia Spanish-funded project. J.S.N. acknowledges a postgraduate fellowship from Conserjería de Innovación Ciencia y Empresa, Junta de Andalucía, Spain. Partial support from CTM2010-21229 (M. of Science and Technology) Spanish-funded project is also acknowledged. NCEP and CMAP data have been provided by the NOAA/OAR/ESRL PSD, Boulder, Colorado, United States, from their website at www.esrl.noaa.gov/psd. ECMWF ERA-Interim data used in this study were obtained from the ECMWF data server. Time series of the teleconnection patterns were retrieved from the NOAA Climate Prediction Center. Comments from three anonymous reviewers were of great help to improve the former manuscript.

REFERENCES

Angelucci, M. G., N. Pinardi, and S. Castellari, 1998: Air–sea fluxes from operational analyses fields: Intercomparison between ECMWF and NCEP analyses over the Mediterranean area. *Phys. Chem. Earth,* **23,** 569–574, doi:10.1016/S0079-1946(98)00071-8.

Barnston, A. G., and R. E. Livezey, 1987: Classification, seasonality and persistence of low-frequency atmospheric circulation patterns. *Mon. Wea. Rev.,* **115,** 1083–1126, doi:10.1175/1520-0493(1987)115<1083:CSAPOL>2.0.CO;2.

Berrisford, P., D. Dee, K. Fielding, M. Fuentes, P. Kallberg, S. Kobayashi, and S. Uppala, 2009: The ERA-Interim archive. ECMWF Tech. Rep. 1, 16 pp. [Available online at http://www.ecmwf.int/publications/library/ecpublications/_pdf/era/era_report_series/RS_1.pdf.]

Bethoux, J. P., 1979: Budgets of the Mediterranean Sea: Their dependence on the local climate and on the characteristics of Atlantic waters. *Oceanol. Acta,* **2,** 157–163.

——, and B. Gentili, 1999: Functioning of the Mediterranean Sea: Past and present changes related to freshwater input and climatic changes. *J. Mar. Syst.,* **20,** 33–47, doi:10.1016/S0924-7963(98)00069-4.

Boukthir, M., and B. Barnier, 2000: Seasonal and inter-annual variations in the surface freshwater flux in the Mediterranean Sea from the ECMWF re-analysis project. *J. Mar. Syst.,* **24,** 343–354, doi:10.1016/S0924-7963(99)00094-9.

Bryden, H. L., and T. H. Kinder, 1991: Steady two-layer exchange through the Strait of Gibraltar. *Deep-Sea Res.,* **38A,** S445–S463, doi:10.1016/S0198-0149(12)80020-3.

Bunker, A. F., H. Charnock, and R. A. Goldsmith, 1982: A note on the heat balance of the Mediterranean and Red Seas. *J. Mar. Res.,* **40,** 73–84.

Castellari, S., N. Pinardi, and K. Leaman, 1998: A model study of air–sea interactions in the Mediterranean Sea. *J. Mar. Syst.,* **18,** 89–114, doi:10.1016/S0924-7963(98)90007-0.

Conte, M., A. Giuffrida, and S. Tedesco, 1989: The Mediterranean Oscillation: Impact on precipitation and hydrology in Italy. *Conference on Climate and Water,* Government Printing Centre, 121–137.

Criado-Aldeanueva, F., J. Soto-Navarro, and J. García-Lafuente, 2012: Seasonal and interannual variability of surface heat and freshwater fluxes in the Mediterranean Sea: Budgets and exchange through the Strait of Gibraltar. *Int. J. Climatol.,* **32,** 286–302, doi:10.1002/joc.2268.

Dai, A., I. Y. Fung, and A. D. del Genio, 1997: Surface observed global land precipitation variations during 1900–88. *J. Climate,* **10,** 2943–2962, doi:10.1175/1520-0442(1997)010<2943:SOGLPV>2.0.CO;2.

Garrett, C., R. Outerbridge, and K. Thompson, 1993: Interannual variability in Mediterranean heat and buoyancy fluxes. *J. Climate,* **6,** 900–910, doi:10.1175/1520-0442(1993)006<0900:IVIMHA>2.0.CO;2.

Gilman, C., and C. Garrett, 1994: Heat flux parameterization for the Mediterranean Sea: The role of atmospheric aerosols and constraints from the water budget. *J. Geophys. Res.,* **99** (C3), 5119–5134, doi:10.1029/93JC03069.

Gomis, D., M. N. Tsimplis, B. Martín-Míguez, A. W. Ratsimandresey, J. García-Lafuente, and S. A. Josey, 2006: Mediterranean sea level and barotropic flow through the Strait of Gibraltar for the period 1958–2001 and reconstructed since 1659. *J. Geophys. Res.,* **111,** C11005, doi:10.1029/2005JC003186.

Harzallah, A., D. L. Cadet, and M. Crepon, 1993: Possible forcing effects of net evaporation, atmospheric pressure, and transients on water transports in the Mediterranean Sea. *J. Geophys. Res.,* **98** (C7), 12 341–12 350, doi:10.1029/93JC00376.

Hurrell, J. W., 1995: Decadal trends in the North Atlantic Oscillation: Regional temperatures and precipitation. *Science,* **269,** 676–679, doi:10.1126/science.269.5224.676.

——, and H. van Loon, 1997: Decadal variations in climate associated with the North Atlantic Oscillation. *Climatic Change,* **36,** 301–326, doi:10.1023/A:1005314315270.

——, and C. Deser, 2010: North Atlantic climate variability: The role of the North Atlantic Oscillation. *J. Mar. Syst.,* **79,** 231–244, doi:10.1016/j.jmarsys.2009.11.002.

——, Y. Kushnir, G. Ottersen, and M. Visbeck, Eds., 2003. *The North Atlantic Oscillation: Climate Significance and Environmental Impact. Geophys. Monogr.,* Vol. 134, Amer. Geophys. Union, 279 pp.

Jones, P. D., T. Jonsson, and D. Wheeler, 1997: Extension to the North Atlantic Oscillation using early instrument pressure observations from Gibraltar and south-west Iceland. *Int. J. Climatol.,* **17,** 1433–1450, doi:10.1002/(SICI)1097-0088(19971115)17:13<1433::AID-JOC203>3.0.CO;2-P.

——, T. J. Osborn, and K. R. Briffa, 2003: Pressure-based measures of the North Atlantic Oscillation (NAO): A comparison and an assessment of changes in the strength of the NAO and its influence on surface climate parameters. *The North Atlantic Oscillation: Climate Significance and Environmental Impact, Geophys. Monogr.,* Vol. 134, Amer. Geophys. Union, 51–62.

Josey, S. A., 2003: Changes in the heat and freshwater forcing of the eastern Mediterranean and their Influence on deep water formation. *J. Geophys. Res.,* **108,** 3237, doi:10.1029/2003JC001778.

——, and R. Marsh, 2005: Surface freshwater flux variability and recent freshening of the North Atlantic in the eastern subpolar gyre. *J. Geophys. Res.,* **110,** C05008, doi:10.1029/2004JC002521.

——, S. Somot, and M. Tsimplis, 2011: Impacts of atmospheric modes of variability on Mediterranean Sea surface heat exchange. *J. Geophys. Res.,* **116,** C02032, doi:10.1029/2010JC006685.

Kalnay, E., and Coauthors, 1996: The NCEP/NCAR 40-Year Reanalysis Project. *Bull. Amer. Meteor. Soc.,* **77,** 437–471, doi:10.1175/1520-0477(1996)077<0437:TNYRP>2.0.CO;2.

Kutiel, H., P. Maheras, and S. Guika, 1996: Circulation indices over the Mediterranean and Europe and their relationship with rainfall conditions across the Mediterranean. *Theor. Appl. Climatol.,* **54,** 125–138, doi:10.1007/BF00865155.

Maheras, P., E. Xoplaki, and H. Kutiel, 1999: Wet and dry monthly anomalies across the Mediterranean basin and their relationship with circulation 1860–1990. *Theor. Appl. Climatol.,* **64,** 189–199, doi:10.1007/s007040050122.

Mariotti, A., 2010: Recent changes in the Mediterranean water cycle: A pathway toward long-term regional hydroclimatic change? *J. Climate,* **23,** 1513–1525, doi:10.1175/2009JCLI3251.1.

——, and P. Arkin, 2007: The North Atlantic Oscillation and oceanic precipitation variability. *Climate Dyn.,* **28,** 35–51, doi:10.1007/s00382-006-0170-4.

——, M. V. Struglia, N. Zeng, and K.-M. Lau, 2002: The hydrological cycle in the Mediterranean region and implications for the water budget of the Mediterranean Sea. *J. Climate,* **15,** 1674–1690, doi:10.1175/1520-0442(2002)015<1674:THCITM>2.0.CO;2.

Matsoukas, C., A. C. Banks, N. Hatzianastassiou, K. G. Pavlakis, D. Hatzidimitriou, E. Drakakis, P. W. Stackhouse, and I. Vardavas, 2005: Seasonal heat budget of the Mediterranean Sea. *J. Geophys. Res.,* **110,** C12008, doi:10.1029/2004JC002566.

May, P. W., 1986: A brief explanation of Mediterranean heat and momentum flux calculations. NRL Rep. (NORDA Code 322), Stennis Space Center, MS, 7 pp.

Palutikof, J. P., 2003: Analysis of Mediterranean climate data: Measured and modelled. *Mediterranean Climate: Variability and Trends,* H. J. Bolle, Ed., Springer-Verlag, 125–132.

Papadopoulos, V., S. Josey, A. Bartzokas, S. Somot, S. Ruiz, and P. Drakopoulou, 2012a: Large-scale atmospheric circulation favoring deep- and intermediate-water formation in the Mediterranean Sea. *J. Climate,* **25,** 6079–6091, doi:10.1175/JCLI-D-11-00657.1.

——, H. Kontoyiannis, S. Ruiz, and N. Zarokanellos, 2012b: Influence of atmospheric circulation on turbulent air-sea heat fluxes over the Mediterranean Sea during winter. *J. Geophys. Res.,* **117,** C03044, doi:10.1029/2011JC007455.

Peixoto, J. P., M. De Almeida, R. D. Rosen, and D. A. Salstein, 1982: Atmospheric moisture transport and the water balance of the Mediterranean Sea. *Water Resour. Res.,* **18,** 83–90, doi:10.1029/WR018i001p00083.

Pettenuzzo, D., W. G. Large, and N. Pinardi, 2010: On the corrections of ERA-40 surface flux products consistent with the Mediterranean heat and water budgets and the connection between basin surface total heat flux and NAO. *J. Geophys. Res.,* **115,** C06022, doi:10.1029/2009JC005631.

Rogers, J. C., 1984: The association between the North Atlantic Oscillation and the Southern Oscillation in the northern hemisphere. *Mon. Wea. Rev.,* **112,** 1999–2015, doi:10.1175/1520-0493(1984)112<1999:TABTNA>2.0.CO;2.

——, 1990: Patterns of low-frequency monthly sea-level pressure variability (1899–1986) and associated wave cyclone frequencies. *J. Climate,* **3,** 1364–1379, doi:10.1175/1520-0442(1990)003<1364:POLFMS>2.0.CO;2.

——, and H. van Loon, 1979: The see-saw of winter temperatures between Greenland and northern Europe. Part II: Some oceanic and atmospheric effects in middle and high latitudes. *Mon. Wea. Rev.,* **107,** 509–519, doi:10.1175/1520-0493(1979)107<0509:TSIWTB>2.0.CO;2.

Romanou, A., G. Tselioudis, C. S. Zerefos, C. A. Clayson, J. A. Curry, and A. Anderson, 2010: Evaporation–precipitation variability over the Mediterranean and the Black Seas from satellite and reanalysis estimates. *J. Climate,* **23,** 5268–5287, doi:10.1175/2010JCLI3525.1.

Ruiz, S., D. Gomis, M. G. Sotillo, and S. A. Josey, 2008: Characterization of surface heat fluxes in the Mediterranean Sea from a 44-year high-resolution atmospheric data set. *Global Planet. Change,* **63,** 256–274, doi:10.1016/j.gloplacha.2007.12.002.

Serreze, M. C., F. Carse, R. G. Barry, and J. C. Rogers, 1997: Icelandic low cyclone activity: Climatological features, linkages with the NAO, and relationships with recent changes in the northern hemisphere circulation. *J. Climate,* **10,** 453–464, doi:10.1175/1520-0442(1997)010<0453:ILCACF>2.0.CO;2.

Slonosky, V. C., and P. Yiou, 2001: Secular changes in the North Atlantic Oscillation and its influence on 20th century warming. *Geophys. Res. Lett.,* **28,** 807–810, doi:10.1029/2000GL012063.

Supic, N., B. Grbec, I. Vilibic, and I. Ivancic, 2004: Long-term changes in hydrographic conditions in northern Adriatic and its relationship to hydrological and atmospheric processes. *Ann. Geophys.,* **22,** 733–745, doi:10.5194/angeo-22-733-2004.

Suselj, K., and K. Bergant, 2006: Mediterranean Oscillation Index. *Geophysical Research Abstracts,* Vol. 8, Abstract 02145. [Available online at http://meetings.copernicus.org/www.cosis.net/abstracts/EGU06/02145/EGU06-J-02145.pdf.]

Trenberth, K. E., 1984: Signal versus noise in the Southern Oscillation. *Mon. Wea. Rev.,* **112,** 326–332, doi:10.1175/1520-0493(1984)112<0326:SVNITS>2.0.CO;2.

van Loon, H., and J. C. Rogers, 1978: The see-saw of winter temperatures between Greenland and northern Europe. Part I: General descriptions. *Mon. Wea. Rev.,* **106,** 296–310, doi:10.1175/1520-0493(1978)106<0296:TSIWTB>2.0.CO;2.

Walker, G. T., and W. E. Bliss, 1932: World weather V. *Mem. Roy. Meteor. Soc.,* **44,** 53–84.

Xie, P., and P. A. Arkin, 1996: Analysis of global monthly precipitation using gauge observations, satellite estimates, and numerical model predictions. *J. Climate,* **9,** 840–858, doi:10.1175/1520-0442(1996)009<0840:AOGMPU>2.0.CO;2.

——, and ——, 1997: Global precipitation: A 17-year monthly analysis based on gauge observations, satellite estimates, and numerical model outputs. *Bull. Amer. Meteor. Soc.,* **78,** 2539–2558, doi:10.1175/1520-0477(1997)078<2539:GPAYMA>2.0.CO;2.

Yu, L., X. Jin, and R. A. Weller, 2008: Multidecade global flux datasets from the Objectively Analyzed Air-Sea Fluxes (OAFlux) project: Latent and sensible heat fluxes, ocean evaporation and related surface meteorological variables. OAFlux Project Tech. Rep. OA-2008-01, Woods Hole Oceanographic Institution, Woods Hole, MA, 64 pp.